

Feasibility Study of Axially- Extracted Virtual Cathode Oscillator

G. Singh · M. V. Kartikeyan

Received: 23 December 2006 / Accepted: 9 March 2007 /
Published online: 14 September 2007
© Springer Science + Business Media, LLC 2007

Abstract In this paper, we have analyzed the design parameters of the axially - extracted virtual cathode oscillator, which is high-power microwave source based on the concept of the virtual cathode associated with the intense relativistic electrons beam oscillations in the electrostatic potential well. The microwave emission by the virtual cathode oscillator results from both the space and time oscillations of virtual cathode and reflexing electrons trapped in the potential well between the virtual and real cathodes. In the X-band frequency spectrum 700 MW microwave peak power has been obtained analytically by the solid electron beam of 300 kV and 20 kA for feasible design parameters. The analysis has been performed by 2-dimensional, relativistic, electromagnetic particle-in-cell simulation code XOOPIC.

Keywords Virtual cathode · Relativistic electron · Wide-bandwidth · Electron trapping · Space-charge limiting current

1 Introduction

The space-charge of the electrons beam imposes an upper limit on the current in the relativistic vacuum microwave sources and thereby prevents the full utilization of the capabilities of the high-current accelerator [1]. The approach, which appears most promising for making use of entire current of the beam formed in the high-current accelerators and enhancing the efficiency of the emission is to excite the microwave oscillations in a system with the virtual cathode. A distinctive feature of such systems is existence of emission only at the electron current above the limiting values, at which the conditions for the formation of a virtual cathode holds. The system with a virtual cathode can thus be used to develop new high-

G. Singh (✉)
Department of Electronics and Communication Engineering,
Jaypee University of Information Technology, Solan 173215, India
e-mail: drghanshyam.singh@yahoo.com

M. V. Kartikeyan
Department of Electronics and Computer Engineering, Indian Institute of Technology,
Roorkee 247667, India

power, genuinely high-current relativistic microwave devices. One of the devices of this kind is the virtual cathode oscillator [2–5]. The high-power microwaves sources are being developed for applications in controlled nuclear fusion plasma heating, high energy particle accelerator, radar, and many other industrial and military.

Among the several types of pulsed high-power microwave generators, the virtual cathode oscillator has been considered very attractive because of its conceptual and mechanical simplicity, high output power capability [1–19] and possible wide-bandwidth with frequency tunable characters which make it attractive for applications where the high-power and wide-bandwidth is acceptable. This device is based on a special class of the bremsstrahlung radiation of the relativistic electrons oscillating axially in the electrostatic fields [4, 5]. The virtual cathode oscillators have been built in two basic geometries. In one configuration, the microwave extraction is perpendicular to the electron beam (radial extraction), and the other configuration is axially symmetric, the microwave power is extracted in the same direction as the electron beam (axial extraction) [4, 5, 7]. The tunability of the radiation frequencies in virtual cathode oscillator can be achieved by changing the anode-cathode gap spacing, cathode dimensions and shape, and anode voltage with respect to cathode voltage [19]. It does not necessarily need the external applied magnetic field, eliminating the magnetic coils and their power supply which greatly saves volume, weight and cost [10]. It has potential to generate microwaves power ranging from few tens of MW up to a few tens GW in the centimeter to millimeter wavelength range [2–5].

The virtual cathode oscillator can meet all the required characters of the ever-increasing demands of applications except for its low efficiency. Hence recent efforts on virtual cathode oscillators have been focused on studying the basic mechanism of this device and how to improve its efficiency. The researchers [20, 21] have been trying to increase the efficiency of the devices by using the coaxial interaction structure. The principle of generating microwave radiation in virtual cathode oscillator is conceptually simple however the interaction between the electron beam and RF wave is highly nonlinear and complicated. For this reason, there has been no straightforward theory that can provide a whole picture of the device. Without theoretical assistance, it is very difficult to set the goal for experimental study and it is not easy to find the right direction for system optimization. We have emphasized on the feasibility study of axially extracted virtual cathode oscillator in X-band frequency spectrum because most of the experimental and theoretical research of axially extracted virtual cathode oscillators are reported below this frequency band. In this paper, we have tried to understand the basic mechanism of axially extracted virtual cathode oscillator for the feasible design parameters in X-band frequency spectrum. The simulations have been performed using a locally modified XOOPIC 2-dimensional electromagnetic particle-in-cell (PIC) code. Its original version included a variety of features, such as relativistic particle push, field emission, interaction of particle with materials surfaces, and an advance graphical interface with multiple diagnostic [22].

The organization of the paper is as follows. The Section 2 discusses the microwave generation mechanism of the virtual cathode oscillator. The Section 3 describes the simulation model of the axially extracted virtual cathode oscillator. The Section 4 concerned with the simulation results. Finally, Section 5 concluded the work.

2 Concept of virtual cathode oscillator

In the virtual cathode oscillator, high-current relativistic electrons beam generated by the cold cathodes of pulse length ranging from tens to hundreds of nanosecond, propagates into a

region in which the space-charge depression limits the current to a lower value [4, 5, 18–26], that is achieved by sudden increase in the radius of a cylindrical metal drift tube (waveguide) containing a beam propagating at the space-charge limiting current [24–26]. The high negative potential on the cathode generates space-charge limited field emission / explosive electron emission from it. The electrons are accelerated by the anode potential and pass through the anode foil into the cylindrical waveguide (drift tube) as shown in Fig. 1. If the injected beam current exceeds the so-called the space-charge limiting current, the kinetic energy of the some of the electrons is reduced to zero due to the potential depression, and a virtual cathode of the electrostatic potential barrier is formed, which will reflect the incoming electrons [19, 22–25]. The potential barrier called the virtual cathode which is formed at the position where the kinetic energy of the electrons approaches zero.

The position of the virtual cathode and the ratio of the beam to reflection current depend very strongly on the electron energy. Therefore, if the electron energy is modulated at the given frequency, both the virtual cathode position and reflected beam current will oscillate at the same frequency [4, 9–11, 23]. The electrons energy can be modulated by an electromagnetic field and the same field may interact with the modulated reflection current because they have the same frequency. In this interaction, if the phase relation is such that the electromagnetic field obtains energy from the modulated current, result will be field amplification by the virtual cathode oscillation. It is obvious that the amplitude of the beam current modulation and strength of the electromagnetic field are very important to the beam-wave interactions [4, 5, 23].

In general, the virtual cathode is formed at distance from anode that is different from the anode-cathode gap spacing. As a result of the positive potential on the anode, the electrons do not leave the system but rather oscillate between the real and virtual cathodes [1–15]. The microwave emission is attributed to the phase bunching of the oscillating electrons inside the potential well of the system [2–7]. This bunching is due to the energy dependence of the electron oscillation frequency. For the idealized parabolic potential well, the electron oscillation frequency is the function of energy only for the relativistic electrons. In the presence of an oscillatory electric field $E=E_0 \cos(\omega t)$ of frequency $\omega \geq \omega_0$ (electron oscillation frequency), a sample of initially uniformly distributed electron will be bunched.

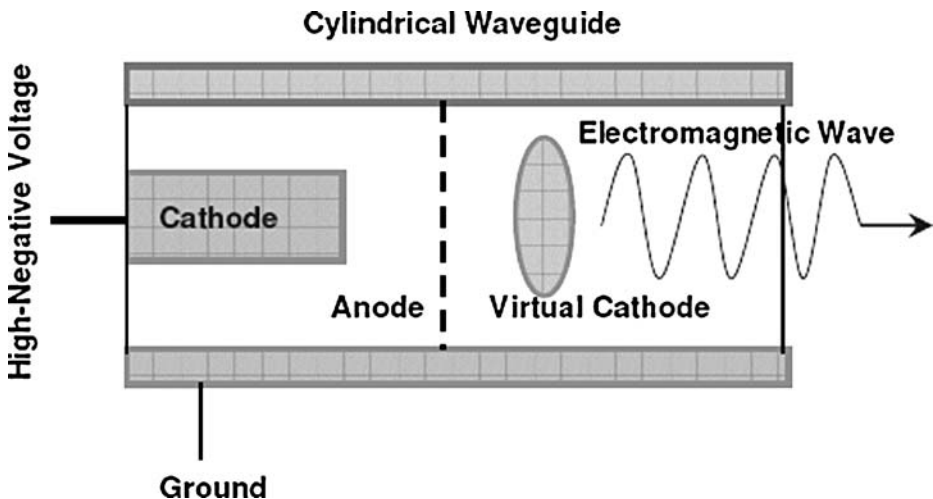


Fig. 1 The schematic of the axially-extracted virtual cathode oscillator.

The reason for this bunching is $\partial\omega/\partial E < 0$ [7]. This nonisochronic mechanism is similar to that of the electron cyclotron maser.

During the electron beam pulse length, there can be a substantial variation in the electron density, and subsequently causes a large change in the oscillation frequency [7]. The frequency usually sweeps from a low to high value during the pulse, because the electron beam current increases due to the partial electron beam diode impedance collapse (closure) [2, 4, 7, 24]. The impedance match between the pulse power driver and the diode affects the power flow to the diode. Any mismatch between the two will produce a variation in the beam current. The systematic impedance drop that occurs during diode closure both increases the beam current and impedance mismatch to the diode. The electron beam current variation can be significant with short pulses of hundreds nanosecond or less simply because as the pulse gets shorter, the rise and fall time become a large fraction of the beam pulses. In the case of the virtual cathode oscillator, the availability of the convenient high power, high voltage, and low impedance electron beam generator plays a key role [18, 23].

2.1 Space-charge limiting current

The space-charge limiting current is the beam current at which the electrostatic potential energy exceeds the kinetic energy of the beam and defined by the beam energy and the cylindrical metal drift tube (waveguide) geometry [18, 19, 22–26]. The electrons cross the anode-cathode gap and pass through the anode foil into the waveguide, a potential depression is generated at the center of the guide [2–7]. The current is high enough so that the depression exceeds driving the anode-cathode potential. Above the space-charge limit, no stable steady state for the electron beam exists [23]. Instead, the beam experiences a jump instability, whereby it transit from a stable steady state to an oscillatory, but non-etheless stable equilibrium. When beam current is greater than the space charge limiting current, the injected electron beam split into two parts, the transmitted beam and reflected beam, near the virtual cathode where the potential is close to cathode potential. For high-voltage diode the magnitude of the potential minimum is negligible compared with the high-applied potential [3–7]. In this case the location of the potential minimum is practically coincident with the cathode surface [23]. Hence, it may be assume that the electric field vanishes at the cathode surfaces and that the emitted electrons have zero initial velocity, in which case the velocity of the electron at any position between the electrodes is determined from the conservation of energy. This is essentially the characteristic of the space charge limited flow [4–5, 23].

For the case of mildly relativistic electron beam, an interpolate formula for the space charge limiting current (I_{sc1}) in the cylindrical waveguide that has good experimental agreement is [1–7, 21, 25]:

$$I_{sc1} = 17(\gamma^{2/3} - 1)^{3/2} / (1 + 2 \ln(r_w/r)) \cdot (\text{kA}) \quad (1)$$

where $\gamma = (1 + V(kV)/511)$ is the relativistic factor of the electron and V is the anode potential with respect to cathode. r_w and r are the radius of the cylindrical waveguide (drift tube) and electron beam, respectively. In general, it is difficult to determine when a virtual cathode will form; the space charge limiting currents depends on the initial beam energy and current density profile as well as the details of the evacuated volume boundary.

2.2 Microwave generation mechanism

The virtual cathode oscillator without a resonant structure is a free-running oscillator. The microwave output frequency of the free-running virtual cathode oscillator varies between

the frequencies ($\omega_p^{rel} \leq \omega_{osc} \leq \sqrt{2\pi}\omega_p^{rel}$), where $\omega_p^{rel} = (4\pi n e^2 / \gamma m)^{1/2}$ is the electron plasma frequency, n and m are the electron density and mass, respectively. The value of $\sqrt{2\pi}$ is an empirical result, which has not yet been derived theoretically. The value of virtual cathode oscillation frequency ω_{osc} increases with the current monotonically. It is important to note that maximum gain occur at $(5/2)\omega_p^{rel}$. Thus the waves at frequencies other than $(5/2)\omega_p^{rel}$ may grow if the virtual cathode oscillation configuration allows feedback at those frequencies as in the case of resonant cavity [2–7].

The microwave emission frequency from the virtual cathode oscillator is usually explained by two dynamical mechanisms [1–17]: first is by the oscillating virtual cathode in the space and time with a well-defined period. This oscillation results in severe longitudinal charge bunching and second mechanism is the trapping of the electrons in the potential well formed between the real and virtual cathodes. The electrons reflexing in this potential well generate broadband microwave power at a higher frequency than in the case of the oscillating virtual cathode, because the individual reflexing electrons can travel at near the speed of light, whereas, the frequency of the virtual cathode oscillations is determined by the plasma frequency of the electron beam. The electron reflection due to the virtual cathode and its frequency f is given by $f=1/4T$, where T is the transit time of electrons to move back and forth between the cathode and anode. The transit time is given by $T = \int dz/v$, where v is the electron velocity and d is the distance between the anode and cathode.

In the microwave generation mechanism by the virtual cathode oscillation, the oscillating electric field modulates the electron energy of the injected beam and extract energy from the current oscillation of the reflected beam. The virtual cathode plays the role of converting the energy modulation of the injected beam to the current modulation of the reflected beam [11]. It has been common recognition that the microwave emission was attributed to the phase bunching of the reflexing electrons inside the potential well formed between the cathode and virtual cathode as well as oscillation of the virtual cathode itself, both mechanisms coexist in the virtual cathode oscillator [8–11]. For the reflexing mechanism, the phase bunching of the reflexing electrons is due to the energy dependences of the electron reflex frequency [4–5]. This process need a small initial energy spread of the electrons and a stable shape of the potential well. However, high-efficiency microwave generation needs large amplitude of the density modulation of electrons, which by space-charge effect results in unstable potential well distribution. In addition, interactions of the electrons with electromagnetic waves give rise to energy spread of the electrons that are trapped in the potential well. Consequently, the virtual cathode oscillator relying on the reflexing mechanism is not applicable for the high-efficiency [8–11], narrow-bandwidth microwave generation. Furthermore, due to the large energy spread of the electrons trapped by the potential well, the reflexing movement is harmful to the virtual cathode oscillator.

2.3 Mode of microwave radiation

In both the mechanism of microwave radiations (virtual cathode oscillation in the space and time and electron trapped into potential well between the real and virtual cathodes) causing the axial electric field E_z to vary between the anode and virtual cathodes in the oversized cylindrical waveguide [4–6]. This couples naturally into the axially symmetric transverse magnetic waveguide modes (TM_{0n}). If the cold injected electron beams are azimuthally symmetric, the only non-zero fields are: E_z , E_r and B_θ in the cylindrical waveguide geometry, which define the transverse magnetic (TM) waves [4–7]. The preferred waveguide mode for an axially-symmetric electrons beam in the smooth-wall cylindrical waveguide is TM_{0n} , where $n = D/\lambda$, D is the waveguide diameter and λ is the free-space wavelength. The free-

space wavelength depends upon the guide dimensions and geometry [4, 5]. The preferred mode appears to be near cutoff that is lower order modes. Thus D/λ should be chosen close to an integer value. The microwave emission mode from virtual cathode oscillator is analyzed by calculating the axial electric field E_z . The transverse magnetic modes possess on axial electric field that strongly couples to the oscillating virtual cathode electric field. In addition, TM modes have circumferential magnetic field at the wall. This magnetic field can be used for coupling the output waveguide structure to the waveguide (drift tube) through the circumferential slots [7]. This configuration has the important advantage of coupling the microwave power from the drift tube by exciting the dominant TE_{01} in the rectangular output waveguide. This allows an unambiguous measurement of output power using conventional waveguide diagnostics because this mode of propagation in the waveguide is well characterized.

3 Simulation model

In simulation of the axially-extracted virtual cathode oscillator, the diameter and length of the cylindrical cathode are 4 cm and 2 cm, respectively. The anode is of aluminum foil of thickness $12\ \mu\text{m}$. For optimum power and frequencies in X-band, the anode-cathode gap is kept at 5 mm where as the variation of the spacing has taken from 0.1 cm to 1.0 cm in the analysis. The drift tube (cylindrical waveguide) length and diameter is 50 cm and 9.8 cm, respectively. The simulation model of the axially-extracted virtual cathode oscillator is shown in Fig. 1. The cutoff frequency of the waveguide corresponding to this dimension for TM_{01} mode is 2.35 GHz. The input parameters of the diode are 300 kV of 70 ns rectangular pulse duration of rise time 10 ns as shown in Fig. 2.

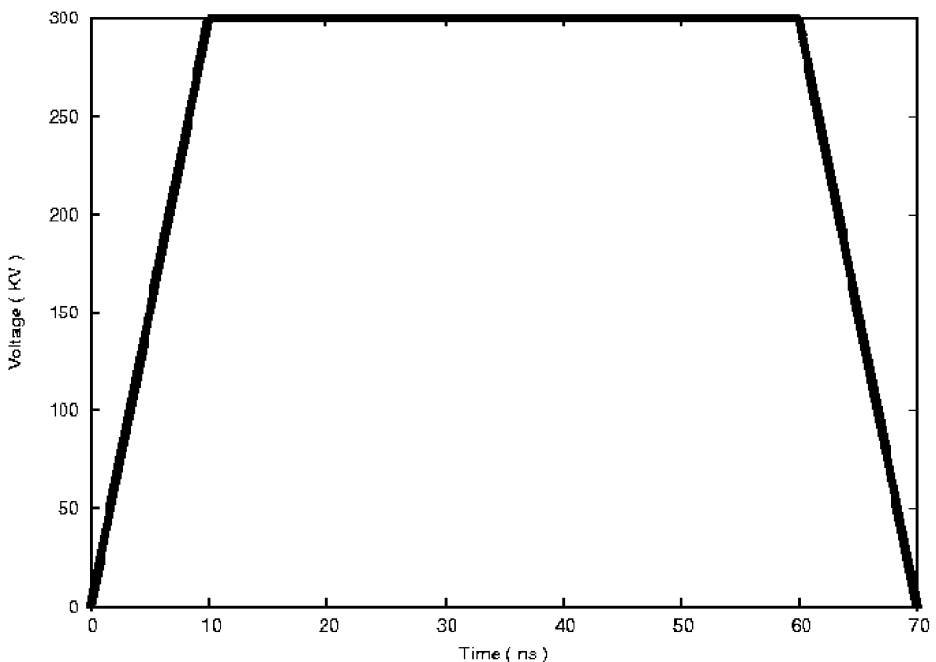


Fig. 2 Schematic of the voltage pulse on the cathode for simulation model.

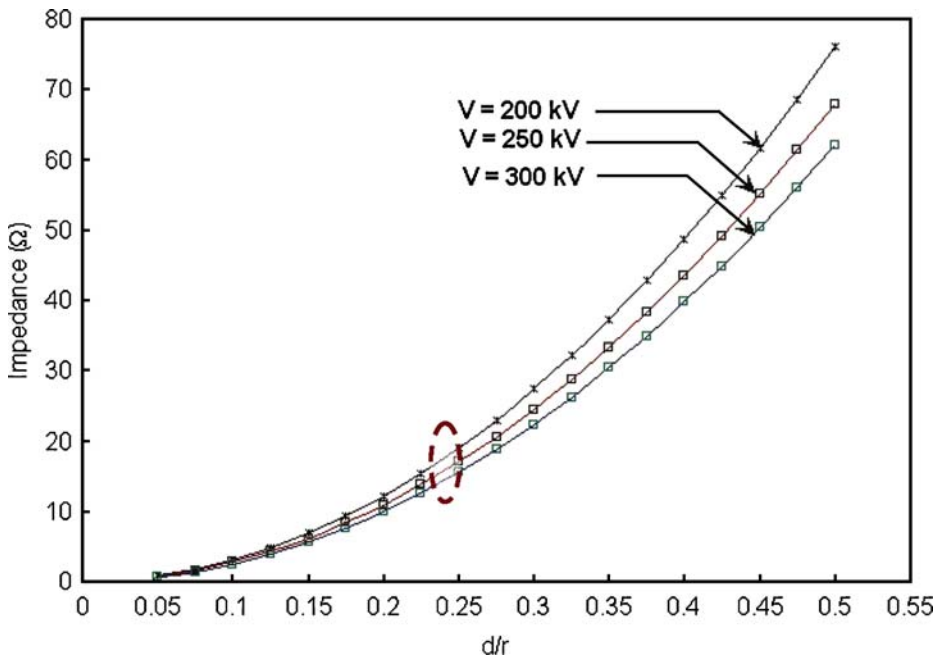


Fig. 3 Variation of the impedance of diode of the axially-extracted virtual cathode oscillator with the ratio of anode – cathode spacing with radius of the solid electron beam, taking the anode voltage with respect to cathode voltage as parameter. The waveguide (drift tube) radius and solid electron beam radius is 4.9 cm and 2.0 cm, respectively.

The incident voltage is fixed and the current caused by the incident voltage calculated by simulation code. We have used a self consistent model for electron emission, because we are working above the space charge limiting current. We use the local electric field at each point on the cathode for calculating the local current density using the Child’s-Langmuir’s law with an emission threshold zero eV. At the exit point for electromagnetic wave, we have used surface impedance boundary condition for the electromagnetic field as described in [22]. The surface impedance boundary conditions are employed to reduce the solution volume during the analysis of scattering from lossy dielectric object. The surface impedance boundary condition in finite difference time domain method is to reduce the computational resource requirements for modeling highly conducting lossy dielectric objects. In the standard FDTD method, modeling highly conducting lossy dielectric objects requires that the cell size be chosen small enough to resolve the field inside the object at the maximum frequency of the interest. The cell size must be chosen as some fraction of the wavelength inside the conducting material at the maximum frequency of interest.

4 Simulation result

From the Child-Langmuir relation, it has been known that exceeding the limiting current of diode leads to the development of a virtual cathode. Its oscillation can generate high-power microwave. The Burkhart *et al.* [7] already has reported that the electron beam impedance below 10 Ω in virtual cathode oscillator never produced microwave. In contrast, the good results were nearly always obtained for beam impedances in between 10 to 20 Ω , below

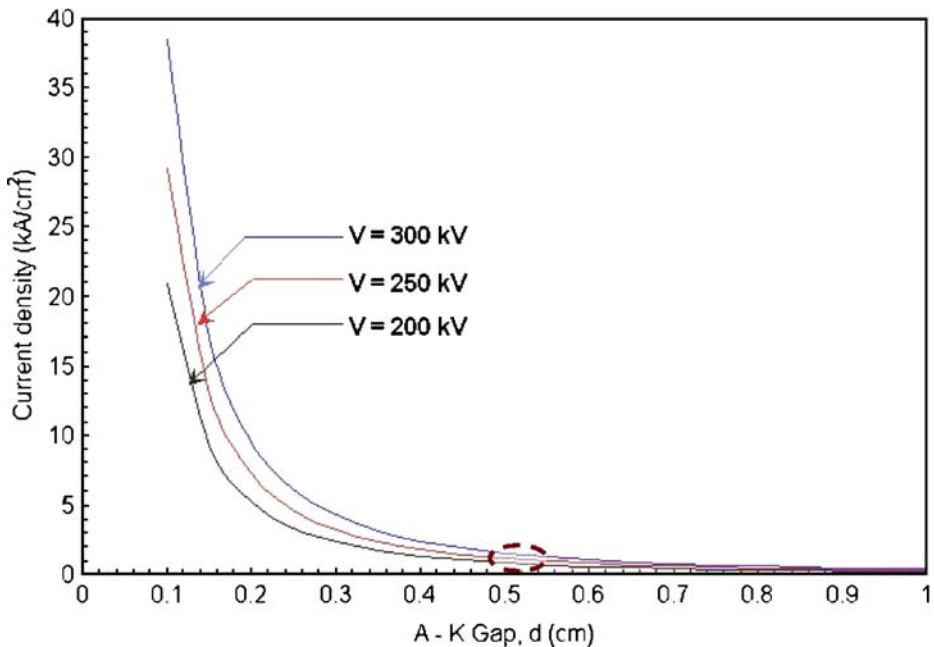


Fig. 4 The variation of the electron beam current density with anode - cathode spacing of the diode of the axially-extracted virtual cathode oscillator, taking anode voltage with respect to cathode voltage as parameter. The drift tube radius and solid electron beam radius is same as in Fig. 3.

10 Ω beams would be tending to pinch from the self magnetic field and above 30 Ω it would expand. The beam impedance depends upon the cathode radius, anode-cathode gap spacing, and anode voltage with respect to cathode voltage as shown in Fig. 3.

The electron reflexing in the potential well between virtual and real cathode creates a reverse current which raise the diode impedance. The impedance of the diode of the axially extracted virtual cathode oscillator at 300 kV cathode voltage and 0.5 cm anode-cathode spacing is 15.6 Ω (as marked in Fig. 3). This impedance is optimized with respect to output microwave power. It is desirable that the impedance of the diode matched as closely as possible to the impedance of the pulse forming network in order to maximize the power flow. For virtual cathode formation, beam current must be greater than the space-charge limiting current as given by (1). The electron beam current density variation with anode-cathode spacing, taking the anode voltage (with respect to cathode voltage) as parameters is shown in Fig. 4. The electron beam current calculated by the simulation code (1.60 kA/cm²) at 300 kV cathode voltage with 0.5 cm anode-cathode spacing as marked in the Fig. 4. The resistive losses are small, so the only major loss is due to the diode mismatch where the power is reflected back down the input transmission line.

The output microwave frequency of the axially extracted virtual cathode oscillator can be tuned by varying the current density or energy (voltage) of the electron beam and the spacing between the real and virtual cathodes. As the anode-cathode gap spacing decreases the spacing between the anode and virtual cathode is also reduced thus, higher frequencies are expected at lower anode-cathode gap spacing as shown in Fig. 5. The frequency of the microwave generated by the virtual cathode oscillations and the electron trapping phenomenon in the axially extracted virtual cathode oscillator is 9.88 GHz and 11.65 GHz respectively, at 300 kV cathode voltage with 0.5 cm anode-cathode gap spacing as marked in the Fig. 5. This

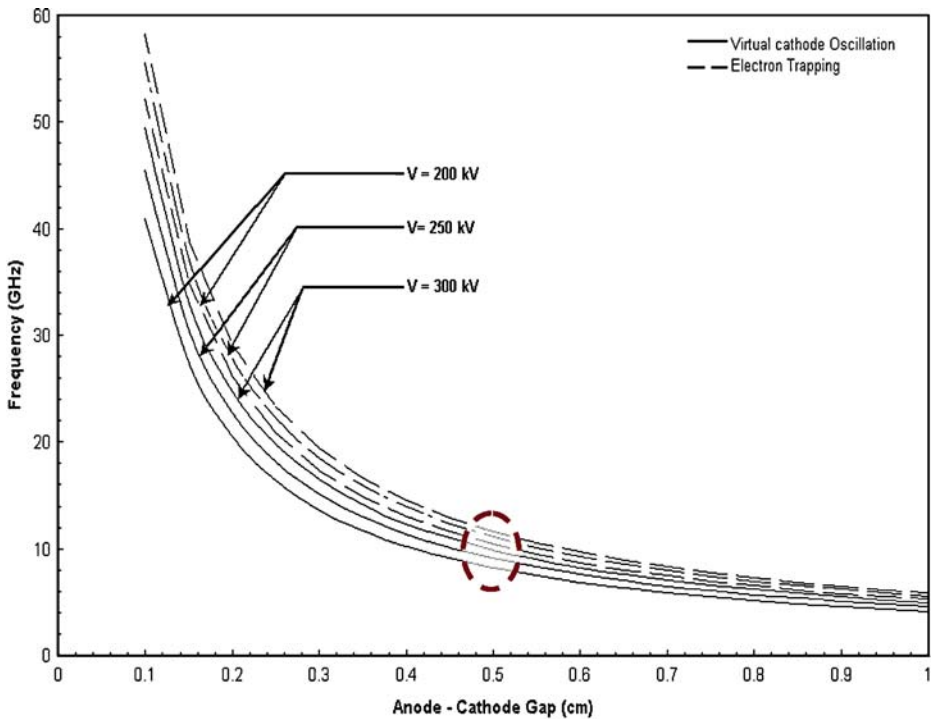


Fig. 5 The variation of the axially-extracted virtual cathode oscillation frequency with anode – cathode spacing, taking the anode voltage with respect to cathode voltage as parameter. The drift tube radius and solid electron beam radius is same as in Fig. 3.

frequency spectrum is in X-band. The center frequency of the spectrum is varies with the square root of the time averaged anode potential. For very small gap spacing the current is so large that the associated inductive loss limits the corrected diode voltage below the emission threshold this means beam pinching will form, thereby suppressing the microwave emission. For the gaps that are greater than 1 cm, the current transmitted through anode foil is insufficient to create a virtual cathode due to electron beam expansion.

The virtual cathode oscillator prefers certain frequencies of operation. Thus for efficient operation at different frequencies, the diode and waveguide dimension must be changed along with the input voltage. The virtual cathode oscillator frequency and power vary with cathode radius; by reducing the cathode radius would increase the electron density and the electron plasma frequency, so the oscillation frequency will change. It also changes the electron beam impedance that is the most important features for virtual cathode oscillator. The frequency of this modulation depends on the density of the oscillating electrons, the applied voltage and geometry of the system. Primarily, the density of passing electrons, their energy and the constitution of the diode determines the modulation amplitude. The smaller anode-cathode gap spacing is shown to shift the frequency up (Fig. 5) while simply changing the cathode diameter had a small effect on the frequency shift. The frequency band of the optimized operation is in X-band. At the frequency of the oscillation of the virtual cathode that is the same as the frequency of the oscillation of the electrons as well as the modulation frequency of passing electron stream [1]. The observed bandwidth in the virtual cathode oscillator is 16% of center frequency, where the bandwidth is defined as the difference between the highest and the

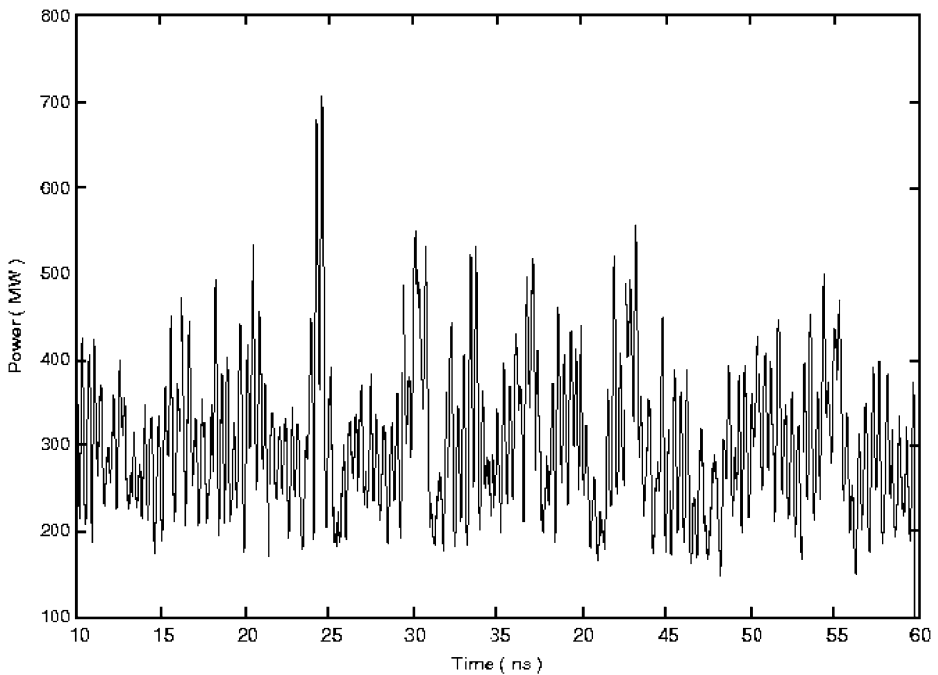


Fig. 6 The variation of the out put microwave power from the axially-extracted virtual cathode oscillator with time (ns) of the voltage pulse. The drift tube radius and solid electron beam radius is same as in Fig. 3. The anode voltage with respect to cathode is 300 kV, rise and fall time are 10 ns each, and flat time is 50 ns.

lowest frequency during the pulse divided by the center frequency. This bandwidth corresponds to the optimized operation in X-band. The frequency usually sweep from low to high value during the pulse because the electron beam current increases due to partial electron beam diode impedance collapse. Typically, the frequency of the virtual cathode oscillator varies because of the diode voltage variation, ion formation [13, 14] and diode closure velocities. However, the frequency variation is not a basic property of the virtual cathode microwave devices itself. Rather, the frequency variations appear to be associated with the pulsed power generator used to energize the diode.

The output peak microwave power generated by the axially-extracted virtual cathode oscillator is as shown in Fig. 6. The frequency of the highest microwave power spectrum (700 MW) is in the X-band. The microwave output associated with the axially-extracted virtual cathode oscillator is found to very complex. The virtual cathode oscillator pulse shows a spike structure superimposed on a slower varying envelop. The simplest explanation of this spike structure is mode competition in the waveguide downstream of the virtual cathode. The downstream conducting structure is usually large compared with wavelength; so many modes can be excited. The frequencies are time dependent and the power is often distributed among a number of modes, thus causing spiky or modulated output. It results, in lower gain and lower efficiency for two reasons. First, gain bandwidth product of the given device with fixed load is a constant. The virtual cathode oscillator tends to have larger bandwidth and moderate gain. The second reason, which is related to the first, is that the frequency change so rapidly that the instability does not saturates, and maximum gain is never obtained as result. In the absence of any downstream resonant structure, the bandwidth of the virtual cathode oscillator is large because of several factors like — non-uniform voltage, anode - cathode gap closure

and transverse beam energy. Since the frequency depends on voltage and anode-cathode gap, the bandwidth is similarly dependent on these two quantities. Beam temperature is also an important parameter that creates bandwidth because the transverse components of the electron energy do not interact with the virtual cathode. Beam temperature is produced both by the emission process and by scattering in the anode foil. It also reduces the emission efficiency. The result of the above variation is chirping of microwave frequency. The strongest chirping occurs at the highest frequencies, where the gap-closure is proportionately larger. The reason for low efficiency is not well understood, it has been speculated that the ion formation, electron beam pinching, or diode gap-closure may also be responsible for the loss in output microwave power. The power, frequency, and pulse width are all sensitive to the cathode shape, and the frequency depends strongly on the anode-cathode gap spacing. Also, the frequency output depends strongly on the anode-cathode spacing. We have found theoretically that the optimal spacing corresponded to the best matching of the virtual cathode oscillator diode impedance and its high voltage feed-line wave impedance. The frequency of the oscillating virtual cathode oscillator scales with current density. The diode aspect ratio must be maintained to reduce the impedance and keep the electrical current above the magnetic insulation limits [25]. Therefore virtual cathode oscillator increases in size as the operating frequency decreases.

5 Conclusion

The axially-extracted virtual cathode oscillator is a high-power, broadly tunable, and broadband microwave source. At 300 kV and 70 nanosecond rectangular voltage pulse of rise and fall-time 10 nanosecond with the anode-cathode gap spacing is 0.5 cm, generate the 700 MW microwave peak power. The frequency of the microwave emission is in X-band (9.88 – 11.65 GHz) with bandwidth of 16% of central frequency. This analysis has been performed by particle-in-cell code - XOOPIC. We have emphasized on feasibility study of axially extracted virtual cathode oscillator in X-band frequency of electromagnetic spectrum because most of the experimental and theoretical research are reported below this frequency band. The ability of the oscillating virtual cathode to produce very high levels of peak-power leads one to consider it as a candidate for controlled nuclear plasma heating, high energy particle accelerator, radar, and many other industrial and military applications.

Acknowledgment The authors are sincerely grateful to Professor Dr. T. S. Lamba (Dean Academic and Research) for valuable discussion and suggestions. The authors are also thankful to the reviewer for critical comments and suggestions to improve the quality of the manuscript.

References

1. V. P. Grigor'ev, A. G. Zherlisyn, S. L. Kuznetsov, and G. V. Mel'nikov, Mechanism for the emission of electromagnetic radiation in system with a virtual cathode, *Sov. J. Plasma Phys.* **14**, 118–121, (1988).
2. D. J. Sullivan, High power microwaves generation from a virtual cathode oscillator (VIRCATOR), *IEEE Trans. Nucl. Sci.* **30**, 3426, (1983).
3. T. J. T. Kwan, High-power coherent microwave generation from oscillating virtual cathode, *Phys. Fluids* **27**, 228–232, (1984).
4. J. Benford and J. Swegle, *High-Power Microwaves* (Artech House: Boston, 1992).
5. V. L. Granatstein and I. Alexeff, *High-Power Microwave Sources* (Artech House: Boston, 1987).
6. R. A. Mahaffey, P. Sprangle, J. Golden, and C. A. Kapetanacos, High-power microwaves from nonisochronic reflecting electron system, *Phys. Rev. Lett.* **39**, 843–846, (1977).
7. S. C. Burkhart, R. D. Scarpetti, and R. L. Lundberg, A virtual cathode reflex triode for high-power microwave generation, *J. Appl. Phys.* **58**, 28–36, (1985).

8. H. Sze, J. Benford, T. Young, D. Bromley, and B. Harteneck, A radially and axially extracted virtual cathode oscillator (viricator), *IEEE Trans. Plasma Sci.*, **13**, 492–497, (1985).
9. T. J. T. Kwan, Formation of virtual cathodes and microwave generation in relativistic electron beams, *Phys. Fluids* **27** 1570–1572, (1984).
10. S. A. Kitsanov, A. I. Klimov, S. D. Korovin, I. K. Kurken, I. V. Pegel, and S. D. Polevin, A viricator with electron beam premodulation based on high current repetitively pulsed accelerator, *IEEE Trans. Plasma Sci.* **30**, 274–284, (2002).
11. W. Jiang, K. Masugata, and K. Yatusi, Mechanism of microwave generation by virtual cathode oscillator, *Phys. Plasmas* **2**, 982–986, (1995).
12. W. Jiang and M. Kristiansen, Theory of virtual cathode oscillator, *Phys. Plasmas* **8**, 3781–3787, (2001).
13. A. E. Dubinov, I. A. Efimova, I. Y. Kormilova, S. K. Saikov, V. D. Selemir, and V. P. Tarakanov, Nonlinear dynamics of electron beams with a virtual cathode, *Physics of Particles and Nuclei* **35**(2), 251–284, (2004).
14. A. E. Dubinov, I. Ya Komilova, and V. D. Selemir, Collective ion acceleration in systems with virtual cathode, *Physics-Uspekhi* **45**(11), 1109–1129, (2002).
15. D. Price, D. Fittinghoff, J. Benford, H. Sze, and W. Woo, Operational features and microwave characteristics of the viricator-II experiment, *IEEE Trans. Plasma Sci.* **16**, 177–184, (1988).
16. H. A. Davis, R. R. Bartsch, L. E. Thode, E. G. Sherwood, and R. M. Stringfield, High-power microwave generation from a virtual cathode device, *Phys. Rev. Lett.* **55**, 2293–2296, (1985).
17. W. Y. Yong Woo, Two dimensional features of virtual cathode and microwave emission, *Phys. Fluids* **30**, 239–243, (1987).
18. J. Benford, D. Price, H. Sze, and D. Bromley, Interaction of viricator microwave generator with an enclosing resonant cavity, *J. Appl. Phys.* **61**, 2098–2100, (1987).
19. E.A. Coutsias and D.T. Sullivan, Space-charge limit instabilities in electron beams, *Phys. Rev. A* **27**, 1535–1543, (1983).
20. Q. Xing, D. Wang, F. Huang, and J. Deng, Two-dimensional theoretical analysis of the dominant frequency in the inward-emitting coaxial viricator, *IEEE Trans. Plasma Sci.* **34**, 584–589, (2006).
21. H. Shao, G. Liu, Z. Yang, C. Chen, Z. Song, and W. Huang, Characteristics of modes in coaxial viricator, *IEEE Trans. Plasma Sci.* **34**, 7–13, (2006).
22. J. P. Verboncoeur, A. B. Langdon, and N. J. Gladd, An object-oriented electromagnetic PIC code, *Comp. Phys. Commun.* **87**, 199–211, (1995).
23. M. Yasuzuka, K. Nagakawa, Y. Hashimoto, O. Ishihara, and S. Nobuhara, Electron beam behaviour in an axially- extracted virtual cathode oscillator, *IEEE Trans. Plasma Sci.* **22**, 939–944, (1994).
24. C. K. Birdsall and W. B. Bridges, Space charge instabilities in electron diodes and plasma converters, *J. Appl. Phys.* **32**, 2611–2618, (1961).
25. R. B. Miller, *An Introduction to the Physics of Intense Charge Particle Beam* (New York: Plenum, 1982).
26. L. E. Thode, B. B. Goldfrey, and W. R. Shanahn, Vacuum propagation of solid relativistic electron beams, *Phys. Fluids* **22**, 747–763, (1979).